IEEE Access
Multidisciplinary : Rapid Review : Open Access Journal

Received October 22, 2018, accepted November 7, 2018, date of publication November 21, 2018, date of current version December 27, 2018.

Digital Object Identifier 10.1109/ACCESS.2018.2882502

A Method of Robot Base Frame Calibration by Using Dual Quaternion Algebra

GANG WANG, XIAOPING LIU, AND SONG HAN
School of Automation, Beijing University of Posts and Telecommunications, Beijing 100876, China

Corresponding author: Gang Wang (wg58977@bupt.edu.cn)

This work was supported in part by the Scientific and Innovation Research Funds for the Beijing University of Posts and Telecommunications under Grant 2017RC22 and in part by the Science and Technology Major Project of Beijing under Grant 141100003514003.

ABSTRACT When the robot is required to execute a certain task in the world coordinate system (WCS), it is necessary to find the coordinate transformation between the robot base coordinate system (RBCS) and WCS to enable the high precision motion planning. This paper presents a simple and accurate method that allows a simultaneous computation of the coordinate transformations (i.e., rotation and translation) from WCS to RBCS. Based on the dual quaternion, the robot kinematic model and formulas for calculating the transformation are derived, which allow calculating the rotation and translation simultaneously. Taking the unit dual quaternion as a constraint, the Lagrangian multiplier method is employed to obtain the optimum transformation. Both simulation and experiment results show that higher calibration precision is obtained. The proposed approach has certain reference value and guiding sense for other calibration problems.

INDEX TERMS Calibration, coordinate transformation, robot base coordinate system, world coordinate system, dual quaternion.

I. INTRODUCTION

With the development of robotic applications, higher requirements have been presented on the accuracy and rapidity of robot. For that reason, how to further improve the accuracy of industrial robots is one of the most important topics in robotics field. Especially, when the robot executes a certain task in WCS, such as robot off-line programming [1] or multi-robot coordinating [2], [3], the kinematic trajectory accuracy of the robot is of great importance. Typically, the kinematic trajectory accuracy is defined and evaluated in RBCS. Accordingly, it is necessary to find the coordinate transformation between RBCS and WCS to realize the motion control in one uniform coordinate.

In recent years, approaches to calibrate the robot base frame had been receiving increased attention. According to the situation to coordinate transformation, the calibration methods can be classified into two categories: 1) separable approach, where the rotation and translation of the transformations is calculated in two steps. 2) simultaneous approach, where the rotation and translation of the transformations is calculated at the same time.

Gan and Dai [2] proposed a base coordinate system calibration approach for coordinated multi-robot system, whose procedure is based on robot joint information of a series of handclasp manipulations. In the detailed approach, the rotation matrix can be reached by solving the equation of the form A = XB for the rotation matrix X. After the rotation matrix was obtained, the translation vector can also be solved out by point transformation equations. Extremely similar to the above calculations, quaternion [4], Procrustes Analysis [5] were employed by utilizing the measurement arm. To tackle the base frame calibration problem for mobile robotic drilling, reference [6] proposed a least-squares fitting method that follows a similar strategy of the method in [2] by utilizing the 2D vision system. Although these methods in [2] and [4]–[6] offer some feasible solution to calibrate the coordinate transformation between RBCS and WCS, the main disadvantage of them is the error propagation caused by using point transformation equations to solve rotation and translation in two steps.

In order to overcome the drawback, such simultaneous approaches were developed. Wu and Ren [7] found the transformation from RBCS to WCS by solving a hand eye calibration problem. A closed-form method serves as an initial value finder, and then an iterative method refines the calibration accuracy, which can simultaneously calculate the rotation and the translation part of the coordinate transformation. While the mentioned method can work well, its complexities are limited by the initial criteria. Moreover, it cannot guarantee whether the method converge to the optimal solution or not.

Consequently, it is necessary to find an alternative methodology that not only overcomes the error propagation shortcomings of separable calibration method, but also avoids the complexity of simultaneous method. In both classes of calibration methods, we can find the position of the robot's end-effector is used only because measuring pose is more complicated than that of position and it is fragile to calculate the pose influenced by measurement errors [7]. Actually, most external measurement devices can only measure the end-effector's position, such as coordinate measuring machine (CMM) [8], [9], automatic theodolite [10], ball-bar [11], measurement arm [4], [5], and optical instruments such as laser tracker [12], [13].

To address these problems, we use the dual quaternion as the basis to find the coordinate transformation (i.e., rotation and translation) between the RBCS and WCS. The dual quaternion, as a natural extension of the quaternion, is convenience to represent an arbitrary transformation comprising rotation and translation, which has the advantages (i.e., compactness, non-singularity, computational efficiency) of only using 8 numbers [14]. Based on the [15], it can be easily shown that a dual-quaternion takes less operations to compute a general transform concatenation compared with a matrix, and it possesses the advantages of high precision, quick operation in robotic kinematics. In recent years, dual quaternion have been used not only for robot kinematics [16] but also for a wide range of applications, such as hand-eye calibration [17], navigation [18] and spacecraft attitude control [19].

In this paper, the main contributions is: the dual quaternion algebra is applied to calibrate the robot base frame, which can uniquely deal with the the rotational and translational part of the transformation simultaneously. The proposed method can not only overcome the error propagation shortcoming of separable calibration method completely, but also avoids the complexity of other simultaneous method, thus can improve the accuracy directly. This paper is organized as follows: Section 2 introduces some mathematical preliminaries of quaternion and dual quaternion. Section 3 deduces formulas for calculating the transformation with dual quaternion descriptors. Section 4 presents numerical simulation to demonstrate various features and effectiveness of the proposed calibration method. Some experiments are presented in Section 5 to validate the applicability of the proposed calibration approach to real system. Finally, the paper is accomplished with some concluding comments.

II. MATHEMATICAL PRELIMINARIES

In order to facilitate our discussion later, this section briefly introduces dual quaternion. As the foundation of the dual quaternion, the quaternion concept is defined first. For more details, please refer to the [20]–[22].

A. QUATERNION ALGEBRA

1) DEFINITION

Quaternion was first described by Irish mathematician Sir William Hamilton in 1843 [23] as an extension of plural to a four-dimensional real space $\mathbb{R}^4$. Formally, a quaternion is defined as

$$\boldsymbol{q} = q_1 + q_2\boldsymbol{i} + q_3\boldsymbol{j} + q_4\boldsymbol{k} \tag{1}$$

where $\boldsymbol{i}^2 = \boldsymbol{j}^2 = \boldsymbol{k}^2 = \boldsymbol{ijk} = -1$. Using concise shorthand, a quaternion can be simplified as $\boldsymbol{q} = [s, \boldsymbol{v}]$ where $s = q_1 \in \mathbb{R}$ is a scalar (called scalar part) and $\boldsymbol{v} = [q_2, q_3, q_4] \in \mathbb{R}^3$ is a 3D vector (called imaginary vector part). Obviously, vector quaternion is a quaternion with zero scalar part $\boldsymbol{q} = [0, \boldsymbol{v}]$ while the scalar quaternion is the quaternion with zero vector part $\boldsymbol{q} = [s, \boldsymbol{0}]$.

Given two quaternions $\boldsymbol{q_1} = [s_1, \boldsymbol{v_1}]$ and $\boldsymbol{q_2} = [s_2, \boldsymbol{v_2}]$, some operation properties are presented as

- Addition

$$\boldsymbol{q_1} + \boldsymbol{q_2} = [s_1 + s_2, \boldsymbol{v_1} + \boldsymbol{v_2}] \tag{2}$$

- Multiplication

$$\boldsymbol{q_1} \circ \boldsymbol{q_2} = [s_1 s_2 - \boldsymbol{v_1} \cdot \boldsymbol{v_2}, s_1\boldsymbol{v_2} + s_2\boldsymbol{v_1} + \boldsymbol{v_1} \times \boldsymbol{v_2}] \tag{3}$$

- Conjugate

$$\boldsymbol{q}^* = [s, -\boldsymbol{v}] = [q_1, -q_2, -q_3, -q_4] \tag{4}$$

- Norm

$$\|\boldsymbol{q}\| = \sqrt{\boldsymbol{q} \circ \boldsymbol{q}^*} = \sqrt{\boldsymbol{q}^* \circ \boldsymbol{q}} \tag{5}$$

Specially, if $\|\boldsymbol{q}\| = 1$, $\boldsymbol{q}$ is called a unit quaternion with its inverse $\boldsymbol{q}^{-1} = \boldsymbol{q}^*$. Note that the arithmetic of quaternion multiplication conforms to associative law, but do not conform to commutative law.

2) ROTATIONS WITH QUATERNION

Due to quaternions can describe the spatial rotation in three dimensions, given the unit rotation axis $\boldsymbol{n}$ and rotation angle θ, we can get

$$\boldsymbol{q} = [\cos(\frac{\theta}{2}), \sin(\frac{\theta}{2})\boldsymbol{n}] \tag{6}$$

3D rotation can be achieved by unit quaternion in the form

$$\boldsymbol{X} = \boldsymbol{q} \circ \boldsymbol{x} \circ \boldsymbol{q}^* \tag{7}$$

where $\boldsymbol{x} = [0, \boldsymbol{v_x}]$ is the initial quaternion representing the rigid transform, $\boldsymbol{X} = [0, \boldsymbol{v_X}]$ is the desired quaternion with the resulting transform.

B. DUAL QUATERNION ALGEBRA

1) DEFINITION

As the Clifford algebra, the dual quaternion comprised of two quaternions is denoted as

$$\hat{q} = \hat{s} + \varepsilon\hat{v} \tag{8}$$

where ε is the dual unit similar to the imaginary unit in complex number with its square as zero $\varepsilon^2 = 0$ and $\varepsilon \neq 0$.

Given two dual quaternions $\hat{\boldsymbol{q}}_1 = [\hat{s_1}, \hat{v_1}]$ and $\hat{\boldsymbol{q}}_2 = [\hat{s_2}, \hat{v_2}]$, the operation are defined as:

- Addition

$$\hat{q_1} + \hat{q_2} = [\hat{s_1} + \hat{s_2}, \hat{v_1} + \hat{v_2}] \tag{9}$$

- Multiplication

$$\hat{q_1} \otimes \hat{q_2} = [\hat{s_1} \circ \hat{s_2}, \hat{s_1} \circ \hat{v_2} + \hat{v_1} \circ \hat{s_2}] \tag{10}$$

- Norm

$$\|\hat{\boldsymbol{q}}\| = \sqrt{\hat{\boldsymbol{q}} \otimes \hat{\boldsymbol{q}}^*} = \sqrt{\hat{\boldsymbol{q}}^* \otimes \hat{\boldsymbol{q}}} \tag{11}$$

- Conjugate

$$\hat{\boldsymbol{q}}^* = [\hat{\boldsymbol{s}}, -\hat{\boldsymbol{v}}] \tag{12}$$

Specially, when $\|\hat{\boldsymbol{q}}\| = 1$, we get a unit dual quaternion with $\hat{\boldsymbol{s}}^{\mathrm{T}} \circ \hat{\boldsymbol{s}} = 1$ and $\hat{\boldsymbol{v}}^{\mathrm{T}} \circ \hat{\boldsymbol{s}} = 1$.

2) ROTATIONS WITH DUAL QUATERNION

According to Chasles' theorem in kinematics, general rigid body displacement can be produced by a translation along a screw axis followed by a rotation about that axis [24], we can obtain

$$\hat{\boldsymbol{q}} = \hat{\boldsymbol{s}} + \varepsilon\hat{\boldsymbol{v}} = [\cos(\frac{\hat{\boldsymbol{\theta}}}{2}), \sin(\frac{\hat{\boldsymbol{\theta}}}{2})\hat{\boldsymbol{n}}] \tag{13}$$

where $\hat{\boldsymbol{n}} = \boldsymbol{n} + \varepsilon(\boldsymbol{p} \times \boldsymbol{n})$ is the screw axis, and $\boldsymbol{p}$ is the vector which is perpendicular to the axis $\boldsymbol{n}$. $\hat{\boldsymbol{\theta}} = \boldsymbol{\theta} + \varepsilon(\boldsymbol{d})$ is the dual angle, $\boldsymbol{d}$ is the translation parallel to the axis $\boldsymbol{n}$.

It's noting that in the dual quaternion form the real part $\hat{\boldsymbol{s}} = \boldsymbol{q}_{rot}$ is the quaternion describing the rotation while the dual part $\hat{\boldsymbol{v}} = \frac{\boldsymbol{q}_{trl} \circ \boldsymbol{q}_{rot}}{2}$ being the translation with $\boldsymbol{q}_{trl} = [0, \boldsymbol{v}_{trl}]$. We have $\hat{\boldsymbol{q}} = \hat{s} + \varepsilon\hat{v} = \boldsymbol{q}_{rot} + \frac{1}{2}\varepsilon\boldsymbol{q}_{trl} \circ \boldsymbol{q}_{rot}$. Obviously, the dual quaternion can deal with the rotation and translation simultaneously. For a convenient notation, the formulation for a rigid body transformation in dual quaternion form is given as below

$$\hat{\boldsymbol{X}} = \hat{\boldsymbol{q}} \otimes \hat{\boldsymbol{x}} \otimes \hat{\boldsymbol{q}^*} \tag{14}$$

where $\hat{\boldsymbol{x}}$ is the initial dual quaternion, $\hat{\boldsymbol{X}}$is the desired dual quaternion.

III. KINEMATIC AND BASE FRAME CALIBRATION MODELLING

A. KINEMATIC MODEL BASED ON DUAL QUATERNION ALGEBRA

As a practical method for modelling the forward kinematics, the dual quaternion formalism has some advantages in computational efficiency [15]. To address the forward kinematics of a n-DOF serial robot, it is necessary to know how the dual quaternion formalism is applied to spatial transformation for one single link. For the *ith* link, a complete transformation using the dual quaternion formalism can be expressed as

$$\hat{\boldsymbol{q}}_{(i-1)i} = \boldsymbol{q}_{rot}(X, \alpha_{i-1}) \circ \boldsymbol{q}_{trl}(X, a_{i-1}) \circ \boldsymbol{q}_{rot}(Z, \theta_i) \circ \boldsymbol{q}_{trl}(Z, d_i) \tag{15}$$

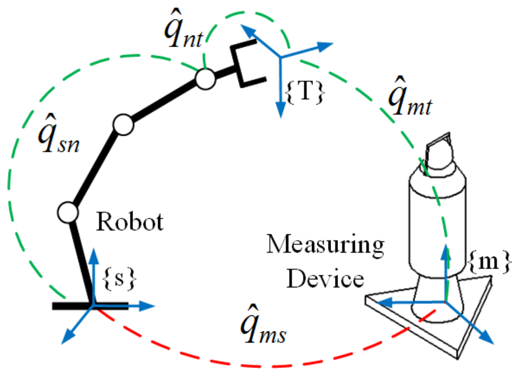

FIGURE 1. Overview of base frame calibration system.

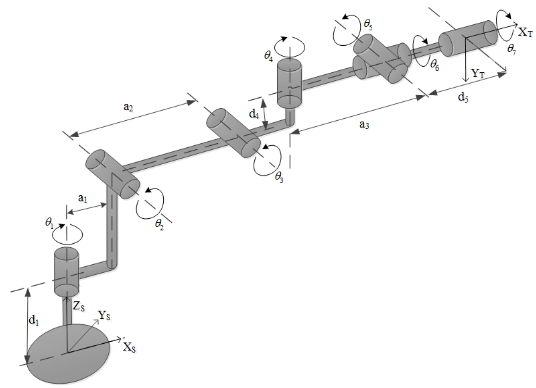

FIGURE 2. Schematic of the 7-DOF robot.

where $\boldsymbol{q}_{rot}(X, \alpha_{i-1})$ denotes the pure rotation about axis $\boldsymbol{X}$ of an angle α_{i-1}, $\boldsymbol{q}_{trl}(X, a_{i-1})$ denotes the pure translation along axis $\boldsymbol{X}$ of distance a_{i-1}, $\boldsymbol{q}_{rot}(Z, \theta_i)$ represent the pure rotation about axis $\boldsymbol{Z}$ of an joint angle θ_i, $\boldsymbol{q}_{trl}(Z, d_i)$ represent the pure translation along axis $\boldsymbol{Z}$ of distance d_i.

For a serial robot, the RBCS is usually fixed to the base link. Here we use {s} as the RBCS, and {t} as the tool coordinate system, as illustrated in Figure 1. Using the dual quaternion theory, the forward kinematics of n-DOF serial robot can be given:

$$\hat{\boldsymbol{q}_{st}}(\boldsymbol{\Theta}) = \hat{\boldsymbol{q}_{s1}} \otimes \hat{\boldsymbol{q}_{12}} \cdots \hat{\boldsymbol{q}_{nt}} \tag{16}$$

where $\boldsymbol{\Theta} = \theta_1, \theta_2 \cdots \theta_n$.

B. ROBOT BADE FRAME CALIBRATION MODEL BASED ON DUAL QUATERNION ALGEBRA

When using the external measuring device to calibrate the base frame, it is obvious the measuring device frame does not coincide with {s}. The WCS {m} is an external reference frame, which is usually defined by the measuring device and attached at the center of it. Let $\hat{\boldsymbol{q}_{mt}}$ be a coordinate transformation relating the position and rotation of the robot end-effector to the world coordinate frame, we have

$$\hat{\boldsymbol{q}_{mt}}(\boldsymbol{\Theta}) = \hat{\boldsymbol{q}_{ms}} \otimes \hat{\boldsymbol{q}_{st}}(\boldsymbol{\Theta}) \tag{17}$$

Since the external measuring device can only measure the position of the end-effector, the mathematics model of robot

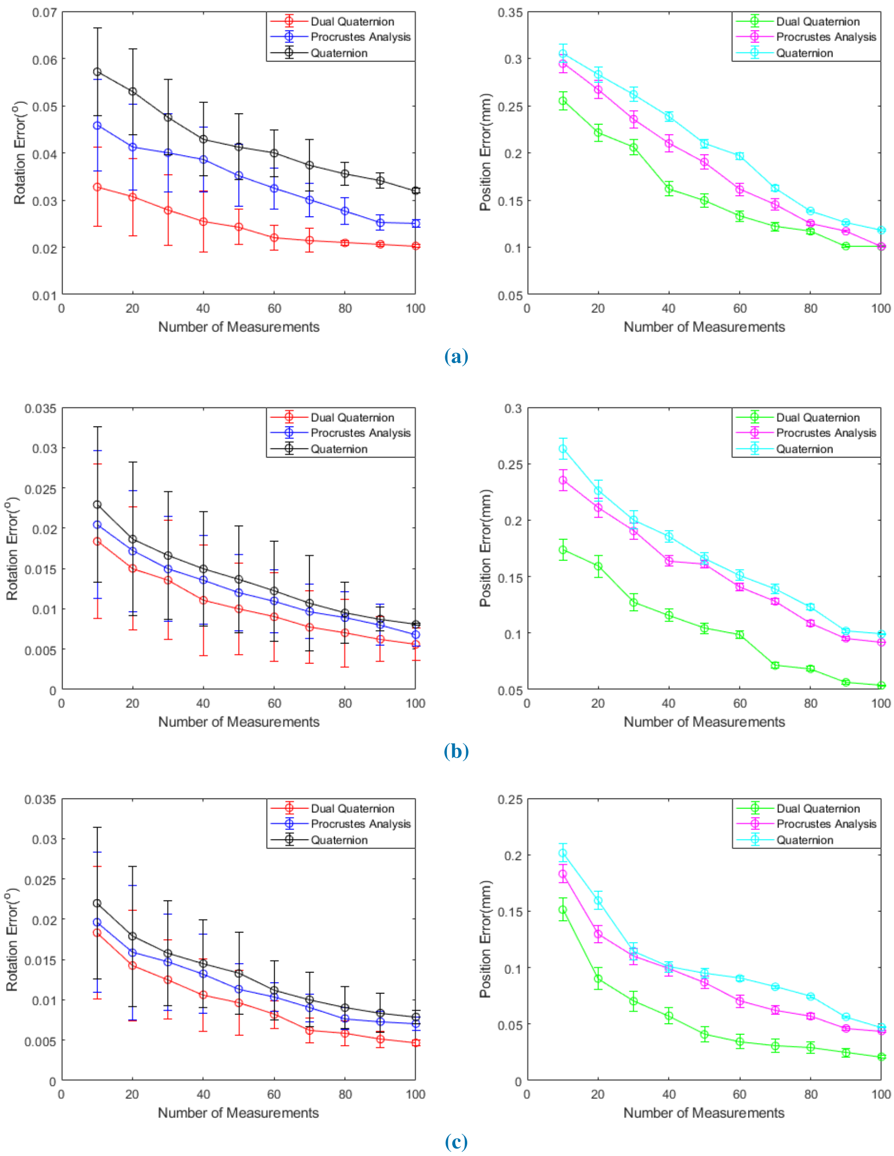

FIGURE 3. (a) Gaussian noise $\sigma = 0.02$, (b) Gaussian noise $\sigma = 0.01$, (c) Gaussian noise $\sigma = 0.005$. Simulation results.

base frame calibration between WCS and RBCS can be expressed as

$$\boldsymbol{p_1} = \hat{q}_{ms} \otimes \boldsymbol{p_0} \otimes \hat{\boldsymbol{q}}_{\boldsymbol{ms}}^* \tag{18}$$

where $\boldsymbol{p_1}$ is obtained from external measuring instrument, $\boldsymbol{p_0}$ is obtained from (16).

The optimization problem is formulated as

$$f(\hat{q_{ms}}) = \frac{1}{N}\sum_{k=1}^{N}\|\boldsymbol{p_1} - \hat{q_{ms}} \otimes \boldsymbol{p_0} \otimes \hat{\boldsymbol{q}}_{\boldsymbol{ms}}^*\| \tag{19}$$

and aims to find the coordinate transformation with the minimum variance, where N is the total joint configuration number, $\|\bullet\|$ represents the Euclidean norm.

Equation (19) can be re-described as

$$f(\hat{s}, \hat{v}) = \frac{1}{N}(\hat{s}^{\mathrm{T}}\boldsymbol{D_1}\hat{s} + \hat{v}^{\mathrm{T}}\boldsymbol{D_2}\hat{s} + N\hat{v}^{\mathrm{T}}\hat{v} + \boldsymbol{D_3}) \tag{20}$$

where

$$\boldsymbol{D_1} = -2\sum_{k=1}^{N}\begin{bmatrix} \boldsymbol{K}(\boldsymbol{p_1})\boldsymbol{K}(\boldsymbol{p_0}) + \boldsymbol{p_1}\boldsymbol{p_0}^{\mathrm{T}} & \boldsymbol{K}(\boldsymbol{p_1})\boldsymbol{p_0} \\ \boldsymbol{p_1}^{\mathrm{T}}\boldsymbol{K}(\boldsymbol{p_0}) & \boldsymbol{p_1}\boldsymbol{p_0} \end{bmatrix}$$

$$\boldsymbol{D_2} = 2\sum_{k=1}^{N}\begin{bmatrix} \boldsymbol{K}(\boldsymbol{p_0})\boldsymbol{K}(\boldsymbol{p_1}) & (\boldsymbol{p_0}) - (\boldsymbol{p_1}) \\ -((\boldsymbol{p_0}) - (\boldsymbol{p_1}))^{\mathrm{T}} & 0 \end{bmatrix}$$

$$\boldsymbol{D_3} = \sum_{k=1}^{N}(\boldsymbol{p_0}^{\mathrm{T}}\boldsymbol{p_0} + \boldsymbol{p_1}^{\mathrm{T}}\boldsymbol{p_1}) = const$$

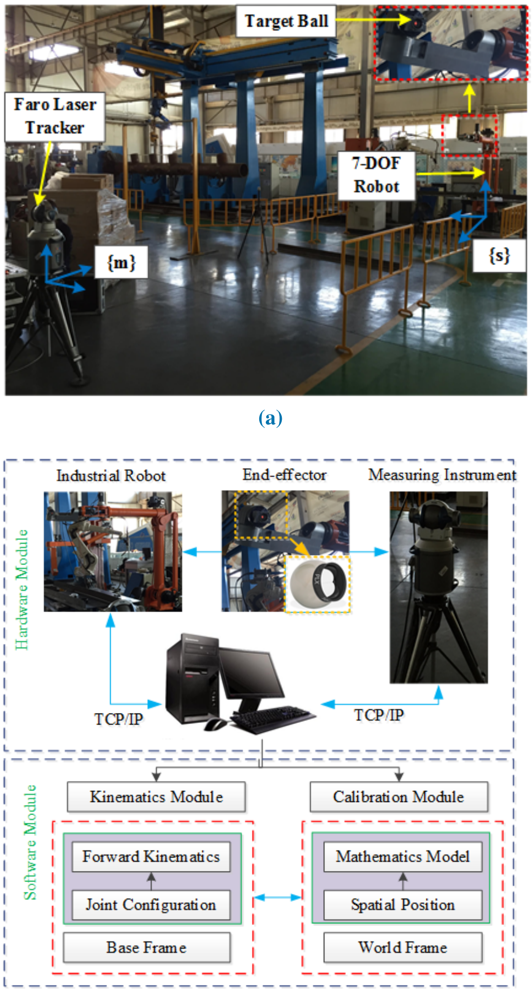

FIGURE 4. (a) Experiment setup with a 7-DOF robot and a FARO laser tracker, (b) Overall architecture of the experiment system. Experiment system.

Considering the constraints of unit dual quaternion, the optimal dual quaternion is obtained by minimizing

$$f(\hat{s}, \hat{v}, \lambda_1, \lambda_2) = \frac{1}{N}[\hat{s}^{\mathrm{T}} \boldsymbol{D_1} \hat{s} + \hat{v}^{\mathrm{T}} \boldsymbol{D_2} \hat{s} + N\hat{v}^{\mathrm{T}} \hat{v} + \boldsymbol{D_3} + \lambda_1(\hat{s}^{\mathrm{T}}\hat{s} - 1) + \lambda_2(\hat{v}^{\mathrm{T}}\hat{s})] \tag{21}$$

where λ_1 and λ_2 is the matrix (unknown) of Lagrange multipliers.

Derivative of $f(\hat{s}, \hat{v}, \lambda_1, \lambda_2)$ with respect to $\hat{s}$ and $\hat{v}$ is as below

$$\frac{\partial f(\hat{s}, \hat{v}, \lambda_1, \lambda_2)}{\partial \hat{s}^{\mathrm{T}}} = \frac{1}{N}[(\boldsymbol{D_1} + \boldsymbol{D_1}^{\mathrm{T}})\hat{s} + \boldsymbol{D_1}^{\mathrm{T}}\hat{v} + 2\lambda_1\hat{s} + \lambda_2\hat{v}] = 0 \tag{22}$$

$$\frac{\partial f(\hat{s}, \hat{v}, \lambda_1, \lambda_2)}{\partial \hat{v}^{\mathrm{T}}} = \frac{1}{N}[\boldsymbol{D_2}\hat{s} + 2N\hat{v} + \lambda_2\hat{s}] = 0 \tag{23}$$

Let us multiply (23) on the left by $\hat{s}^{\mathrm{T}}$

$$\hat{s}^{\mathrm{T}}\boldsymbol{D_2}\hat{s} + 2N\hat{s}^{\mathrm{T}}\hat{v} + \lambda_2 = 0 \tag{24}$$

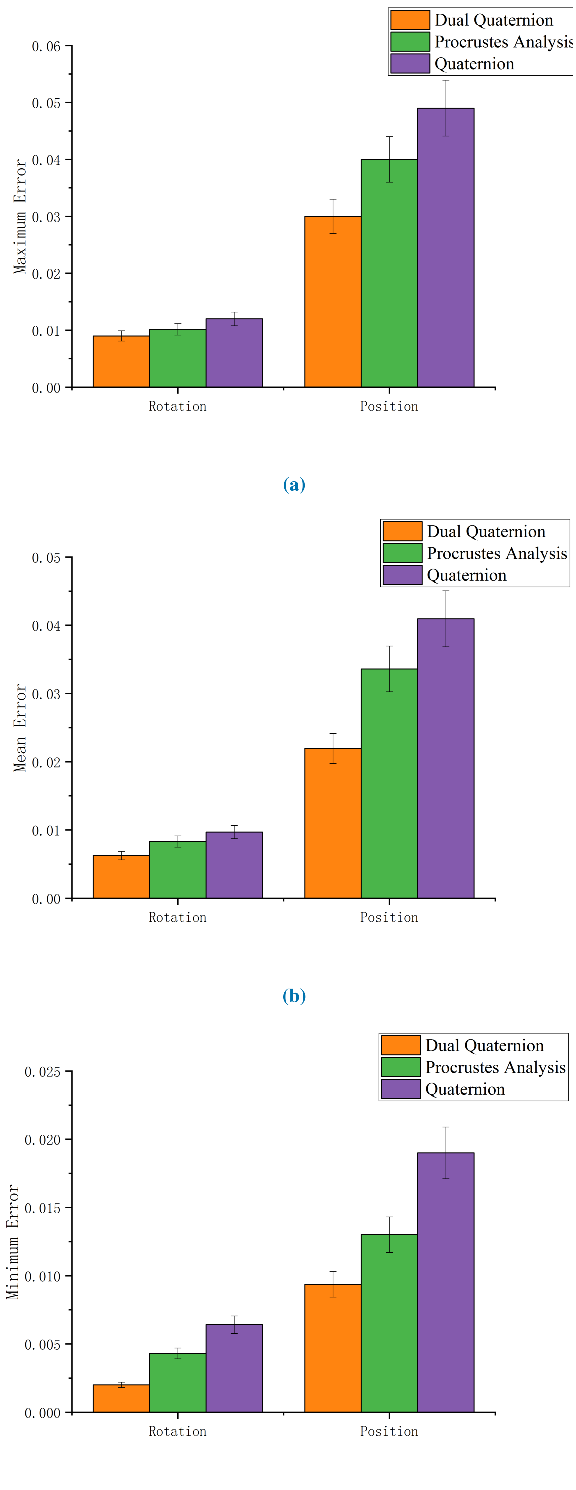

FIGURE 5. (a) Maximum error, (b) Mean error, (C) Minimum error. Verification of calibration results.

As $\boldsymbol{D_2}$ is an anti-symmetric matrix, we can get $\lambda_2 = 0$. Substituting $\lambda_2 = 0$ into (24), we can get

$$\hat{v} = -\frac{\boldsymbol{D_2}}{2N\hat{s}} \tag{25}$$

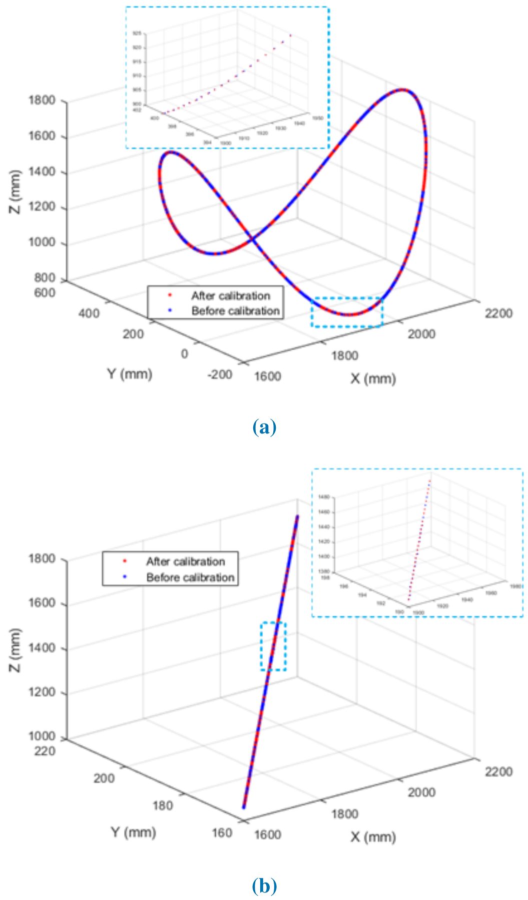

FIGURE 6. **(a) Arbitrary trajectory, (b) Linear trajectory. Trajectory verification.**

Substituting (25) into (22) yields

$$\boldsymbol{A}\hat{\boldsymbol{s}} = \lambda_1 \hat{\boldsymbol{s}} \tag{26}$$

where

$$\boldsymbol{A} = \frac{1}{2}[\frac{1}{2N}\boldsymbol{D_2}^{\mathrm{T}}\boldsymbol{D_2} - (\boldsymbol{D_1}\boldsymbol{D_1}^{\mathrm{T}})] \tag{27}$$

Because of $\boldsymbol{K}(\boldsymbol{p_0})^{\mathrm{T}} = -\boldsymbol{K}(\boldsymbol{p_1})$, $\boldsymbol{K}(\boldsymbol{p_1})^{\mathrm{T}} = -\boldsymbol{K}(\boldsymbol{p_1})$, $\boldsymbol{K}(\boldsymbol{p_0})\boldsymbol{p_0} = -\boldsymbol{K}(\boldsymbol{p_1})\boldsymbol{p_1} = \boldsymbol{0}$, $\boldsymbol{K}(\boldsymbol{p_0})\boldsymbol{p_1} = -\boldsymbol{K}(\boldsymbol{p_1})\boldsymbol{p_0}$, (27) can be expressed as

$$\boldsymbol{A} = \sum_{k=1}^{N}\begin{bmatrix} (\boldsymbol{p_0}(\boldsymbol{p_0})^{\mathrm{T}} + \boldsymbol{p_1}(\boldsymbol{p_1})^{\mathrm{T}})\boldsymbol{I}_{3*3} & 4\boldsymbol{K}(\boldsymbol{p_0})\boldsymbol{p_1} \\ \boldsymbol{0} & (\boldsymbol{p_0}\boldsymbol{p_0}^{\mathrm{T}} + \boldsymbol{p_1}\boldsymbol{p_1}\mathrm{T}) \end{bmatrix} \tag{28}$$

From (28) we can see, quaternion $\hat{\boldsymbol{s}}$ is the eigenvector of a 4-order matrix $\boldsymbol{A}$. Assume λ_1 is the eigenvalue, by plugging (25) and (26) into (21) and rearranging terms, we have

$$f(\hat{\boldsymbol{s}}, \hat{\boldsymbol{v}}) = \frac{1}{N}(\boldsymbol{D_3} - \lambda_1) \tag{29}$$

If we choose the greatest eigenvalue and its eigenvector of matrix $\boldsymbol{A}$, the value of (29) will be minimal. Further, the quaternion $\hat{\boldsymbol{s}}$ can be solved by (28) and $\hat{\boldsymbol{v}}$ by (25). Up to now, we have completed the base frame calibration problem.

IV. SIMULATION

To analyze the performance of calibration method mentioned above objectively, a numerical simulation is carried out for a self-developed 7-DOF serial robot whose schematic and kinematic parameters are shown in Fig. 2 and Table 1.

TABLE 1. **Nominal value of kinematic parameters.**

Link No.	$\alpha_i(°)$	$a_i(mm)$	$d_i(mm)$	$\theta_i(°)$	$Initial\theta_i(°)$
1	0	0	695	θ_1	0
2	90	170	0	θ_2	90
3	0	1350	0	θ_3	-90
4	-90	1150	149	θ_4	90
5	90	0	859	θ_5	90
6	90	0	0	θ_6	-90
7	90	0	0	θ_7	-90

In this part, to compare the performance of the proposed method versus that of the unit quaternion [4] and Procrustes Analysis [5] methods, 100 sets of configurations were generated randomly, and three different levels of Gaussian noise $\sigma = 0.02$, $\sigma = 0.01$, $\sigma = 0.005$ were added to the measurement data. In order to evaluate the accuracy of the proposed solutions, we introduce the rotation error defined as:

$$e_r = \frac{\|\boldsymbol{r} - \boldsymbol{r}'\|}{\|\boldsymbol{r}\|} * 100\% \tag{30}$$

where $\boldsymbol{r}$ and $\boldsymbol{r}'$ are the real value and the estimation value. The unit of error e_r is °. The translation error is defined as:

$$e_t = \frac{\|\boldsymbol{t} - \boldsymbol{t}'\|}{\|\boldsymbol{t}\|} * 100\% \tag{31}$$

where $\boldsymbol{t}$ and $\boldsymbol{t}'$ are the real value and the estimation value, respectively. The error e_t has a unit of length mm.

The simulation results are shown in Fig. 3. It is clear that the performance of three calibration methods with respect to different levels of Gaussian noise is very similar, that is, with measurement number increasing, both the rotation and translation results become more accurate. We can also see that the dual quaternion method performs better than the other two methods, which demonstrates the superiority of dual quaternion uniquely dealing with the rotational and translational part simultaneously. This gives the evidence to verify the theoretical analysis. Under each level of Gaussian noise, the position accuracy in the dual quaternion is almost stable at 40 measurement sets.

V. EXPERIMENT AND RESULT

A. CALIBRATION EXPERIMENT SYSTEM

To verify the effectiveness of the proposed method, representative experiments were conducted using a 7-DOF robot (the same construction with the one in simulation). A laser tracker and an optical target ball were used as a data acquisition source, where the optical target ball was mounted on the end effector and was used to measure the position, as shown in Figure 4. According to the specifications, when the distance

TABLE 2. Robot joint configurations and positions of target ball.

i	Joint Angle(°)							Target Ball Position(mm)		
	θ_1	θ_2	θ_3	θ_4	θ_5	θ_6	θ_7	p_x	p_y	p_z
1	0	0	-0.03	0	73.31	0	-0.03	5640.486	824.632	1590.752
2	-0.56	-2.08	-1.36	-1.97	67.08	-1.27	-8.92	5594.839	893.949	1533.628
3	-10.17	0.93	-4.29	1.12	60.81	1.59	-6.9	5759.874	1187.419	1421.627
4	-13.49	4.45	-6.76	-0.4	65.5	-0.57	-8.3	5885.676	1285.188	1337.816
5	-15.83	1.47	-2.07	-3.34	59.04	5.86	-5.27	5886.068	1439.478	1496.913
6	-18.68	4.52	0.35	-5.87	63.17	8.74	-2.32	6020.880	1521.242	1584.309
7	-16.05	8.93	-1.54	-1.7	66.68	2.89	-7.73	6023.085	1337.022	1511.672
8	-13.29	12.87	-3.29	4.28	61.15	-1.55	-9.91	6032.598	1134.792	1424.569
9	-9.01	14.81	1.6	10.09	56.29	3.21	-7.55	6028.878	900.202	1577.322
10	-5.08	17.18	3	12.24	67.43	1.61	-8.39	6053.549	714.715	1626.925
11	0.69	15.78	-0.36	2.51	70.70	-0.78	-9.56	5988.550	691.030	1525.787
12	-0.96	19.36	-3.93	-0.64	62.48	-3.13	-10.7	6077.579	783.200	1361.191
13	-3.64	13.52	1.03	4.29	67.98	-9.06	-13.64	5945.739	821.951	1585.084
14	-8.87	9.46	4.47	10.07	72.15	-13.6	-15.95	5887.517	929.853	1732.157
15	-12.26	12.78	0.43	5.85	76.46	2.80	-14.46	6014.458	1061.666	1581.843
16	-14.51	17.09	2.4	10.51	79.00	6.67	-12.61	6123.948	1011.359	1627.903
17	-16.82	3.53	-1.17	17.27	83.2	10.64	-10.48	5859.344	1128.692	1570.077
18	-13.42	-1.89	-4.5	18.09	77.25	15.47	-8.04	5718.527	1059.151	1449.533
19	-9.03	-8.82	-6.95	10.78	70.5	10.6	-10.51	5524.137	1069.128	1334.183
20	-4.82	-16.19	-0.44	17.21	63.58	6.06	-12.63	5315.655	862.639	1508.829
21	-0.19	-19.22	3.8	6.63	70.79	-0.67	-16.05	5205.461	826.064	1647.015
22	3.49	-15.18	6.17	0.04	75.83	-4.09	-17.58	5279.853	742.024	1769.233
23	8.71	-8.31	2.18	-6.85	80.14	3.30	3.45	5427.662	601.933	1665.780
24	12.62	-6.00	-0.95	-10.98	75.98	7.68	5.7	5482.371	504.798	1555.438
25	17.66	-6.05	-3.28	-22.89	80.07	11.07	7.39	5505.400	473.458	1483.299
26	13.61	-9.99	0.16	-29.6	76.43	6.87	-1.7	5443.547	734.321	1582.395
27	10.61	-14.63	-1.79	-22.28	71.31	4.09	-3.16	5310.562	763.675	1482.633
28	8.10	-10.19	-4.67	-18.35	65.71	9.27	-5.26	5422.213	810.853	1396.654
29	8.10	-22.23	-4.68	1.05	67.52	5.82	-6.97	5111.124	541.181	1318.153
30	8.10	-25.99	-4.69	11.12	67.52	0.67	-9.51	5042.125	395.888	1283.653
31	2.67	-28.22	-4.7	13.82	74.13	-3.98	-11.85	4998.895	617.996	1271.254
32	-1.95	-28.22	-4.7	19.01	68.04	1.02	-9.21	5042.957	769.605	1263.673
33	-8.14	-32.2	-1.61	21.68	72.36	-2.73	-11.12	5011.398	1049.363	1328.991
34	-3.73	-36.94	-1.08	15.94	74.32	-6.82	-13.59	4863.945	944.825	1286.404
35	-3.73	-31.66	-1.09	21.13	79.71	-11.00	-15.76	4967.270	834.403	1366.816
36	-1.86	-26.81	-1.1	6.44	79.71	10.05	0.83	5071.520	936.495	1419.432
37	-1.43	-22.26	-3.2	3.32	76.41	15.58	11.62	5178.655	942.604	1385.503
38	-1.43	-9.34	-9.1	-6.15	70.47	19.61	16.21	5507.405	1012.655	1255.822
39	3.01	-3.64	-5.69	-6.15	77.54	15.64	14.36	5582.409	808.025	1398.841
40	7.27	-0.07	-1.67	-18.47	75.07	14.56	13.53	5675.039	814.842	1537.403

from laser tracker to robot is less than 10m, the theoretical measurement accuracy of the laser tracker is about 0.022mm, which makes it suitable for measuring the position accuracy and repeatability of serial robots and even calibrating them.

In the data acquisition processing, the robot was programmed to move to 40 configurations randomly, and at the same time, the position of the target ball was measured. Table 2 shows the joint configurations and positions of target ball. Note that, the laser tracker is not displaced and avoids the problem of blocked by other objects during measurement. All measurements with the laser tracker are therefore taken with respect to this world frame.

B. RESULTS AND DISCUSSION

With all the kinematic parameters known and the joint angles input $\boldsymbol{\Theta} = [\theta_1, \theta_2 \cdots \theta_n]$ as well as $[p_{x1}, p_{y1}, p_{z1}]$ given, the transformation from RBCS to WCS can be

$$\hat{\boldsymbol{q}_{ms}} = [0 \quad 0.0002 \quad 0.9943 \quad 0.1054] \circ [0 \quad 640.9 \quad -385.4 \quad -27.4]$$

As we have obtained the transformation, we use the maximum error, mean error and minimum error to further evaluate the accuracy of the calibration results. The experimental result is displayed in Fig. 5, where the unit of the mean rotation error is degrees and the mean position error is mm. The experimental result is in consistence with the simulation result, and quite satisfactory that can meet the requirement for robot base frame calibration.

Up to now, the calibration experiment has been completed. The transformation between RBCS and WCS is identified, we can command the robot to perform any task defined in WCS accurately by transforming the task into RBCS. Besides, we also performed spatial arbitrary trajectory tracking and linear trajectory tracking verification experiment, as illustrated in Fig. 6. At the beginning of the trajectory, the trajectory has a certain deviation due to the sudden start of the 7-DOF robot. In addition, our calibration method is applied in the task space rather than in the joint space, therefore how much freedom of the robot is not important, the results are useful for robots of other mechanical configurations.

VI. CONCLUSION

In this paper, we have proposed a simple and accurate method to calibrate the transformation between the RBCS and WCS. Forward kinematic model has been derived with dual quaternions. Based on it, calibration algorithm for finding the transformation between RBCS and WCS was established by dual quaternion algebra. Because the proposed calibration method based on dual quaternion can uniquely deal with the rotational and translational part simultaneously without decoupling, thus it can avoid error propagation. Consequently, it can be concluded that the calibration method proposed in this paper is especially effective to solve the problem of base frame calibration and it has advantage on easy operation and intensive application value. If we want to further improve the calibration accuracy, our further research will focus on the online kinematic calibration and the dynamic parameters identification. This paper also presents dual quaternion algebra which has a great application foreground in the fields of robot hand-eye calibration and multi-robot base coordinate system calibration, and it could make important contributions to other research.

REFERENCES

[1] Z. X. Pan, J. Polden, N. Larkin, S. Duin, and J. Norrish, "Recent progress on programming methods for industrial robots," *Robot. Comput.-Integr. Manuf.*, vol. 28, no. 2, pp. 87–94, 2012.

[2] Y. Gan and X. Dai, "Base frame calibration for coordinated industrial robots," *Robot. Auton. Syst.*, vol. 59, nos. 7–8, pp. 563–570, 2011.

[3] Y. Gan, X. Dai, and D. Dong, "Robot calibration for cooperative process under typical installation," *J. Appl. Math.*, vol. 2014, Art. no. 576420.

[4] W. Wang, F. Liu, and C. Yun, "Calibration method of robot base frame using unit quaternion form," *Precis. Eng.*, vol. 41, no. 3, pp. 47–54, 2015.

[5] X. Gao, C. Yun, H. Jin, and Y. Gao, "Calibration method of robot base frame using procrustes analysis," in *Proc. Asia-Pacific Conf. Intell. Robot Syst.*, Jul. 2016, pp. 16–20.

[6] B. Mei, W. Zhu, K. Yuan, and Y. Ke, "Robot base frame calibration with a 2D vision system for mobile robotic drilling," *Int. J. Adv. Manuf. Technol.*, vol. 80, nos. 9–12, pp. 1903–1917, 2015.

[7] L. Wu and H. L. Ren, "Finding the kinematic base frame of a robot by hand-eye calibration using 3D position data," *IEEE Trans. Autom. Sci. Eng.*, vol. 14, no. 1, pp. 314–324, Jan. 2017.

[8] M. R. Driels, W. Swayze, and S. Potter, "Full-pose calibration of a robot manipulator using a coordinate-measuring machine," *Int. J. Adv. Manuf. Technol.*, vol. 8, no. 1, pp. 34–41, 1993.

[9] S. A. Kolyubin, L. Paramonov, and A. S. Shiriaev, "Optimising configurations of KUKA LWR4+ manipulator for calibration with optical CMM," in *Recent Advances in Mechanism Design for Robotics*, vol. 33. Cham, Switzerland: Springer, 2015, pp. 189–199.

[10] M. R. Driels and U. S. Pathre, "Vision-based automatic theodolite for robot calibration," *IEEE Trans. Robot. Autom.*, vol. 7, no. 3, pp. 351–360, Jun. 1991.

[11] A. Nubiola, M. Slamani, and I. A. Bonev, "A new method for measuring a large set of poses with a single telescoping ballbar," *Precis. Eng.*, vol. 37, no. 2, pp. 451–460, Apr. 2013.

[12] A. Nubiola and I. A. Bonev, "Absolute calibration of an ABB IRB 1600 robot using a laser tracker," *Robot. Comput.-Integr. Manuf.*, vol. 29, no. 1, pp. 236–245, Feb. 2013.

[13] T. Sun, Y. Zhai, Y. Song, and J. Zhang, "Kinematic calibration of a 3-DoF rotational parallel manipulator using laser tracker," *Robot. Comput.-Integr. Manuf.*, vol. 41, pp. 78–91, Oct. 2016.

[14] J. Xu and K. H. Halse. (2016). "Dual quaternion variational integrator for rigid body dynamic simulation." [Online]. Available: https://arxiv.org/abs/1611.00616

[15] G. Leclercq, P. Lefèvre, and G. Blohm, "3D kinematics using dual quaternions: Theory and applications in neuroscience," *Frontiers Behav. Neurosci.*, vol. 7, no. 7, pp. 1–25, 2013.

[16] E. Özgr and Y. Mezouar, "Kinematic modeling and control of a robot arm using unit dual quaternions," *Robot. Auton. Syst.*, vol. 77, pp. 66–73, Mar. 2016.

[17] B. Busam, T. Birdal, and N. Navab. (2017). "Camera pose filtering with local regression geodesics on the Riemannian manifold of dual quaternions." [Online]. Available: https://arxiv.org/abs/1704.07072

[18] J. Cheng, J. Kim, Z. Jiang, and W. Che, "Dual quaternion-based graphical SLAM," *Robot. Auton. Syst.*, vol. 77, pp. 15–24, Mar. 2016.

[19] A. Valverde, "Dynamic modeling and control of spacecraft robotic systems using dual quaternions," Ph.D. dissertation, Dept. Aeros., Georgia Inst. Technol., Georgia, GA, USA, 2018.

[20] W. R. Hamilton, "On quaternions or on a new system of imaginaries in algebra," *Philos. Mag. J. Sci. Ser. 3*, vol. 25, pp. 10–13, 1844.

[21] M. A. Clifford, "Preliminary sketch of biquaternions," in *Proc. London Math. Soc.*, vol. s1-4, pp. 381–395, Nov. 1873.

[22] E. Study, "Von den bewegungen und umlegungen," *Mathematische Annalen*, vol. 39, no. 4, pp. 441–565, 1891.

[23] J. Denavit and R. S. Hartenberg, "A kinematic notation for lower-pair mechanisms based on matrices," *J. Appl. Mech.*, vol. 22, pp. 215–221, Jun. 1955.

[24] J. M. McCarthy, *Introduction to Theoretical Kinematics*. Cambridge, MA, USA: MIT Press, 1990.

GANG WANG received the B.S. and M.S. degrees in mechanical engineering from the Shandong University of Science and Technology, Shandong, China, in 2006 and 2009, respectively, and the Ph.D. degree in mechanical engineering from Beihang University, Beijing, China, in 2016.

Since 2016, he has been a Lecturer with the Institute of Automation, Beijing University of Posts and Telecommunications, Beijing. His research interests include robot calibration and motion control of mobile robot.

XIAOPING LIU received the B.S., M.S., and Ph.D. degrees in mechanical engineering from Tianjin University, Tianjin, China, in 1988, 1991, and 1994, respectively.

From 1998 to 1999, he was a Visiting Scholar with the University of Washington. He is currently a Professor with the Institute of automation, Beijing University of Posts and Telecommunications, Beijing, China. His research interests include robotics, and fault diagnosis and detection.

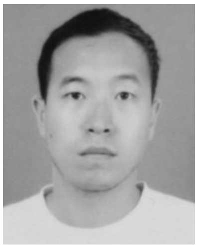

SONG HAN received the B.S. degree from the University of Science and Technology of China, Anhui, China, in 2014. He is currently pursuing the Ph.D. degree with the Automation School, Beijing University of Posts and Telecommunications. His research interests include robot calibration and mobile robot navigation.